A High-Speed Inkjet-Printed Microelectromechanical Relay With a Mechanically Enhanced Double-Clamped Channel-Beam

Seungjun Chung, Muhammed Ahosan Ul Karim, Hyuk-Jun Kwon, William Scheideler, and Vivek Subramanian, *Member, IEEE*

***Abstract*— We report a high-speed inkjet-printed three-terminal microelectromechanical (MEM) relay with a double-clamped beam that exploits the enhanced stiffness of the double-clamped structure to improve electrical performance. To minimize mechanical delay and pull-in voltage, the contact gap between the channel-beam and drain, and the stiffness of the beam and shape of the drain was carefully designed and optimized through a 3-D finite element simulation. The double-clamped beam prevents stiction-related failure between the channel-beam and drain despite the contact gap being only 370 nm for a >500 μm long beam. The resulting printed relay delivers a turn-ON delay of 8 μs at a gate voltage of 10 V, a pull-in voltage of only 7.2 V, immeasurable off-leakage, excellent subthreshold swing, and a small hysteresis window of 2 V without any bending or collapsing of the beam. The device also shows reliable operation over 10^5 cycles while maintaining a high ON/OFF ratio of 10^8, and extremely low ON-state resistance of 3.7 Ω. [2016-0180]**

***Index Terms*— Inkjet-printing, microelectromechanical systems, relays, printed electronics.**

I. Introduction

PRINTED electronics technology is promising for realizing low-cost, low-temperature processed electronic components such as thin-film transistors (TFTs), sensors, organic light-emitting diodes, memory devices for wide ranging applications including displays, sensing systems, and radio-frequency identification tags on large-area and flexible platforms [1]–[6]. Although high-performance inkjet-printed TFTs have been presented with optimized materials for semiconductor, dielectric, and surface modification layers [2], [7], [8], further improvements are still needed with respect to their power-consumption, subthreshold swing, contact resistance and on/off ratio. With this in mind, inkjet-printed micro-electromechanical (MEM) relays have recently attracted interest as a nearly ideal low-power consumption switch that can potentially replace conventional switching devices such as TFTs, delivering extremely low leakage current, subthreshold slope, contact resistance, and excellent on/off ratio [9]–[12]. To make printed MEM relays viable for many applications, the relatively large mechanical delay that limits the maximum switching frequency should be addressed to enable substitution for conventional switching devices such as MOSFETs and TFTs [9], [10]. To improve the switching speed, there are two possible approaches: to increase the gate-overdrive voltage and to scale device dimensions. Although the use of a larger electrostatic force between the gate and channel-beam causes increased acceleration, resulting in faster travel of the beam [9], shortening the travel distance of the channel beam by reducing the actuation and contact gaps (g_o and g_d) is a more direct and effective approach for low-power consumption applications. Unfortunately, reducing the g_d increases the likelihood of collapse of the beam due to stiction forces during sacrificial layer removal. Therefore, the mechanical stiffness of the floated channel beam must be enhanced if the g_d is to be minimized [9]–[11]. A freely suspended beam for highly reliable and robust printed MEM relays without stiction-related failures can be achieved through the optimization of the geometric properties of the beam, for example, by increasing the thickness or shortening the length of the beam, or exploiting the coffee-ring effect to increase its moment of inertia [10], [12]–[15]. These approaches, however, require the use of excessive material, high-resolution patterning, and exquisite control of the coffee-ring barrier; these measures additionally result in a higher pull-in voltage (V_{PI}) [10], [15]. Moreover, MEM relays with cantilever-type single-clamped beams are still susceptible to curling and collapse-related failure if the cantilever beam is not stiff enough to endure stiction or stress-gradient forces at the tip of the beam [11], [14]–[16].Therefore, a robust approach for enhancing the mechanical stiffness using facile printing processes is highly desirable because the mechanical stiffness of the

Manuscript received August 2, 2016; revised September 17, 2016; accepted September 24, 2016. Date of publication November 14, 2016; date of current version February 1, 2017. This work was supported by the Philippine California Advanced Research Institutes (PCARI). S. Chung also appreciates the support from the National Creative Research Laboratory program (Grant 2012026372) funded by the Korean Ministry of Science, ICT & Future Planning. Subject Editor R. T. Howe.

S. Chung was with the Department of Electrical Engineering and Computer Sciences, University of California at Berkeley, Berkeley, CA 94720-1700 USA. He is now with the Department of Physics and Astronomy, Seoul National University, Seoul 08826, South Korea (e-mail: seungjun@phya.snu.ac.kr).

M. A. U. Karim, W. Scheideler, and V. Subramanian are with the Department of Electrical Engineering and Computer Sciences, University of California at Berkeley, Berkeley, CA 94720-1700 USA.

H.-J. Kwon is with the Department of Mechanical Engineering, University of California at Berkeley, Berkeley, CA 94720-1700 USA.

Color versions of one or more of the figures in this paper are available online at http://ieeexplore.ieee.org.

Digital Object Identifier 10.1109/JMEMS.2016.2613877

1057-7157 © 2016 IEEE. Personal use is permitted, but republication/redistribution requires IEEE permission.
See http://www.ieee.org/publications_standards/publications/rights/index.html for more information.

cantilever is quite sensitive to a height of the ridge of the cantilever, a parameter that cannot be controlled easily.

In this study, an inkjet-printed 3-terminal (3T) MEM relay with a double-clamped beam is proposed for the first time to enhance the mechanical stiffness of the beam and give stable and reliable operation with low mechanical delay. In particular, the coffee-ring effect, which can increase the effective thickness of the beam [10], was unnecessary because the double-clamped structure is sufficiently rigid to suspend the beam freely so that the mechanical stiffness of the beam can be more accurately controlled. By optimizing the device geometry, a high-speed printed MEM relay with a freely suspended double-clamped beam was demonstrated that showed lower V_{PI} of 7.2 V, a turn-on delay below 10 μs, a small hysteresis window of 2 V without any bending or collapsing of the beam, and more reliable operation than that of recently reported MEM switches with single-clamped and double-clamped beams, respectively [9], [10], [17]. The operation of the printed MEM relay was also verified and predicted using 3-dimensional (3D) finite element COMSOL Multiphysics simulation.

II. Inkjet-Printed MEM Relay Design

In this work, the inkjet-printed MEM relays were carefully designed to achieve 1) well-defined printed layers, 2) a strongly suspended beam without collapse or curling issues, 3) low-operation voltage below 10 V with feature sizes as small as possible. In these regards, the first consideration is to deliver a mechanical stiffness that is high enough to suspend the beam without collapse- or stiction-related failures during processing. To avoid stiction from the capillary force between the channel-beam and the drain during the sacrificial layer removal, the sticking force should be lower than the spring force of the beam [10], [14],

$$F_{spring} = kx > F_{stiction} = \frac{2A_{contact}\gamma \cos\theta_c}{g - x} \quad (1)$$

where k, x, $A_{contact}$, γ, θ_c, and g denote the spring constant, the beam displacement, the contact area between the beam and the drain, the surface tension of IPA, the contact angle between IPA and printed drain, the contact gap, respectively. Here, the contact width (~ 100 μm) and length (1 μm) were fixed by the minimum beam-width without any waviness or bulging and the ridge created from the coffee-ring effect, respectively to minimize stiction force as shown in Figure 1. Since $A_{contact}$ (~ 100 μm^2) and g (~370 nm) which is the consistent thickness of the sacrificial layer were already determined, the spring constant should be over 7.22 N/m to achieve this requirement. The highly suspended beam was carefully designed to have a spring constant just exceeding 7.22 N/m, because an excessively stiff beam requires a high V_{PI} resulting in a higher pull-in delay [19].

$$V_{PI} = \sqrt{\frac{8}{27}\frac{k_{eff}g_o^3}{\varepsilon_o A_a}} \quad (2)$$

where g_o, ε_o and A_a denote the actuation gap, the vacuum permittivity, and the actuation area (i.e., channel-beam to gate overlap), respectively. Note that a length of the beam (~ 550 μm) was determined with a consideration of margin for the both anchoring parts and the dimension of the underlying layers (a width of the gate (~ 200 μm) and drain electrodes (~ 50 μm). The MEM relay design parameters were summarized in Table 1.

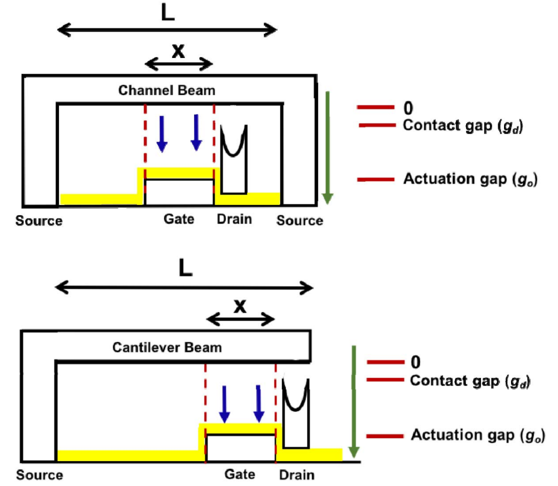

Fig. 1. Schematics of structures for spring constant calculation with fixed-fixed (top) and fixed-free beams (bottom).

TABLE I

Measured and Extracted Parameters of the Printed MEM Relay

Parameter	Value
Gate width	180 µm
Channel width	100 µm
Channel length	530 µm
Thickness of beam	2.6 µm
E_r of printed silver film	41 Gpa
Thickness of drain	0.5 µm (center) + 0.5 µm (edge)
Actuation gap	Air-gap 0.85 µm & PVP 0.45 µm
Contact gap	0.37 µm

It is clear that the designed double-clamped beam results in a much higher effective spring constant (k_{eff}) (calculated - 7.28 N/m) than that of an equivalently sized single-clamped cantilever type beam (calculated – 0.13 N/m), as shown below in the equations (Equation. (3) and (4) show the effective spring constant for the single-clamped cantilever type beam and the double-clamped beam, respectively) relating beam dimensions and Young's modulus of the beams to stiffness (Figure 1) [13]. This approach is, thus, very suitable to realize high-stiffness beams without requiring use of excessively thick structures, which are difficult to form using printing techniques [10].

$$k_{eff_single} = \frac{24EI}{6(L-x)L^2 + x^3 + 2L^3} \quad (3)$$

$$k_{eff_double} = \frac{384EI}{(2L-x)x^2 + 2L^3} \quad (4)$$

Here, E, I, L, and x denote Young's modulus, the momentum of inertia, the length of the beam, and the actuation length by the bottom gate electrode, respectively.

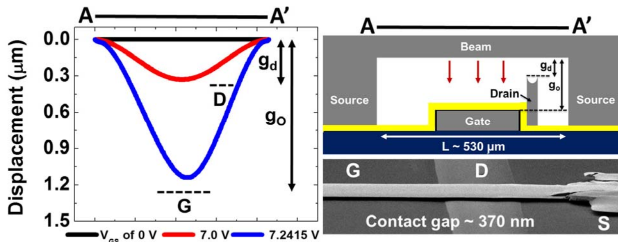

Fig. 2. The simulation results by finite element method (FEM) for the displacement of the beams with respect to the applied electrical field: The channel contacts on the drain with high aspect ratio for gate voltage near V_{PI} of 7.2 V (Schematic of the MEM relay and magnified SEM image focused on the channel and the drain clearly shows the g_d is much smaller than the actuation gap (g_o).

III. Simulation

Figure 2 shows the numerically predicted results of the displacement for the designed printed beam simulated using COMSOL Multiphysics with an AC/DC modules turned on for electrostatic analysis. The bending of the beam was coupled with the electrostatic force between the gate and the beam generated by the electric field in the analysis. Here, we assumed that air surrounded both ends of the double-clamped beam, and that the electrostatic force acted in a direction which is normal to the lower boundary of the beam. The displacement represented the position (in *xz*-plane) at which the elastic restoring force of the beam and the electrostatic force are in equilibrium. The computation was repeated until the channel beam bent beyond the measured g_d of 370 nm (consistent with that measured experimentally by a nanoindentor. It will be discussed in detail later); the gate voltage is V_{PI} when the beam touches the drain. Note that a SEM image clearly also shows that g_d is smaller than g_o due to thickness of the drain with high aspect ratio. Simulations thus provide the value of predicted V_{PI} as 7.2415 V.

IV. Inkjet-Printed MEM Relay Fabrication

Figure 3 shows the double-clamped beam fabrication process flow. For the gate electrode, a commercial silver nanoparticle (AgNP) ink having a particle diameter size of ∼ 70 nm (EMD 6503 from Sunchemical Corp.) was inkjet-printed on a cleaned silicon dioxide substrate and then sintered at 180 °C for 30 min on a hot-plate in air. The gate electrode had a thickness and sheet resistance of 400 nm and 0.6 Ω/sq, respectively. A solution of poly-4-polyvinylphenol (PVP) consisting of 10 wt% PVP and 2 wt % poly(melamine-coformaldehyde) as a cross-linking agent in propylene glycol methyl ether acetate (PGMEA) was spin-coated to form a gate dielectric layer and then cross-linked for 30 min on a 200 °C hot-plate, resulting in a film thickness of 450 nm to isolate the gate electrode from the movable channel beam in cases when the deflection of the beam caused full-contact with the surface. Source and drain electrodes were also inkjet-printed using the same ink and process as for the gate electrode. They were then sintered for 30 min at 180 °C on a hot-plate. Note that the drain was printed in 3 passes on a heated substrate at 60 °C without interspersed drying to increase

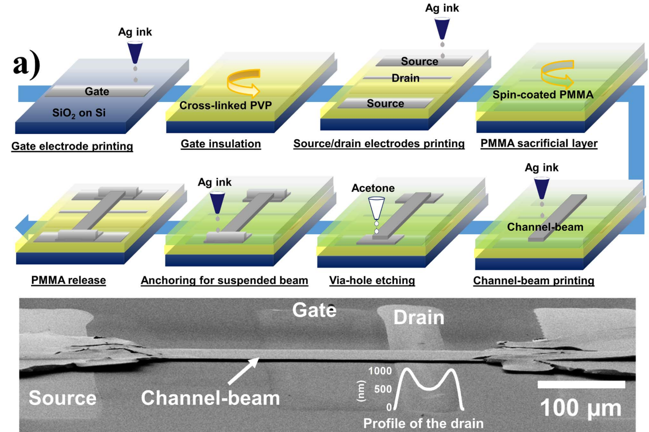

Fig. 3. (a) Schematics of the process flow used to fabricate a MEM relay with a double clamped beam. (b) Profiles of a printed beam on 60 °C PMMA surface depending on printing passes.

the aspect ratio by preventing ink spreading, producing a minimized g_d between the channel beam and drain. The silver nanoparticle ink was printed in a liquid state; a U-shaped printed electrode can be produced intentionally without the need for any additional etching or patterning through appropriate printing and drying conditions due to the coffee-ring effect. This approach exploits the outward flow of the nanoparticles during solvent evaporation, resulting in a highly concentrated silver ridge (∼ 500 nm) [10], [18]. On the bottom electrodes, poly(methyl methacrylate) (PMMA A11 from MicroChem Corp.) was spin-coated at 2000 rpm to form a uniform sacrificial layer and cured at 180 °C for 10 min. On the 1 μm thick PMMA sacrificial layer, the movable channel beam was printed using the same ink as for the bottom electrodes. This was printed in 7 passes without any surface treatments while maintaining the substrate temperature at 60 °C to prevent spreading of the ink. Note that the PMMA sacrificial layer was slightly etched by the solvent of the silver ink during the beam printing, so a dip was observed in the profile. By optimizing substrate temperature and surface energy of the bottom layer, the 7-pass-printed beam had an effective thickness of 2.6 μm which can deliver a minimum mechanical stiffness to prevent the mechanical collapse of the beam by stiction force after consideration of the coffee-ring effect and

a width of 100 μm, as shown in Figure 3b [10]. Afterward, the printed beam was sintered with a ramping condition of 2 °C/min up to 180 °C to realize a thick film without cracking or bulging. The anchor region used to connect the floating beam was etched by printing acetone on both sides of the edges of the beam through the PMMA sacrificial layer. For facile etching, the PMMA sacrificial layer was exposed to ultraviolet ozone (UVO) for 8min before defining the via-hole. Then, the via-hole was filled by printing the same AgNP ink in multiple passes. The filled Ag ink was dried at 125 °C for 30 min for solidification and then sintered up to 180 °C with a ramping condition of 5 °C/min to minimize the damage to the PMMA. Finally, the PMMA sacrificial layer was removed by sequentially dipping the device in boiling acetone and room-temperature isopropyl alcohol (IPA) to release the beam, then dried on a 150 °C hot-plate to complete the relay fabrication. The electrical properties of the printed MEM relay were measured using a semiconductor parameter analyzer (4156C, Agilent Technologies) in air. The thicknesses and surface profiles of the printed electrodes were measured using a surface profilometer (Dektak 6M, Veeco) and a white light interferometry (Wyko NT3300, Veeco). A FEI Nova NanoSEM 650 was used to obtain the scanning electron microscope (SEM) images. The mechanical stiffness of the beam and the printed silver films were measured using a TI 900 TriboIndenter system. All fabrication and measurements were executed in air.

V. Electrical and Mechanical Characteristics Measurements

Figure 4a shows the measured drain current (I_{DS}) versus gate voltage (V_{GS}) characteristics of the printed MEM relay with the double-clamped beam. The gate was placed beneath the middle of the beam and the drain was placed as close as possible to the gate to minimize the V_{PI}, because displacement of the beam in the middle is relatively larger than that of the beam near the edge. Note that since the double-clamped beam will be deformed symmetrically during the operation downward, the placement of the drain on one side of the gate does not affect the electrical performance. The drain formed with a high aspect ratio ensures turn-on operation with low V_{PI} before the channel beam touches the bottom-gate by reducing the g_d. This novel approach to realize the minimized contact region is similar to the dimple structures utilized in conventional microelectromechanical systems (MEMS), but is only feasible with the inkjet-printing process. A high *on/off* ratio at V_{DS} of 0.1 V with immeasurable *off*-state current (the noise floor of our measurement system), abrupt-switching with extremely low-subthreshold swing below 5 mV/dec, and a V_{PI} of 7.2 V with a standard deviation of 0.21 V were maintained throughout an endurance test of up to 10^5 cycles (Figure 4a). which agrees well with the value of predicted V_{PI} as 7.2415 V. We note that this excellent electrical performance is comparable to that of conventional silicon MEM relays [20]–[23]. After 200 k cycles of operation, the V_{RL} was shifted in the negative direction due to welding by joule-heating between the channel and drain that causes an increase in the effective

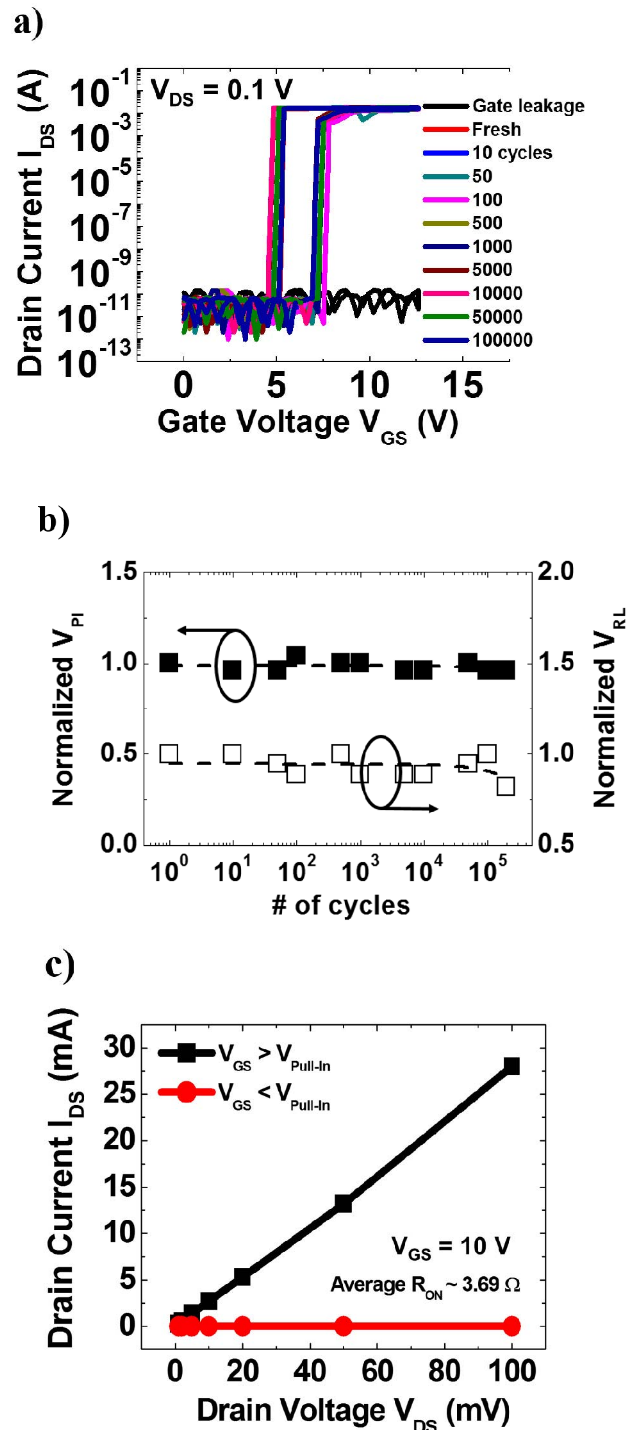

Fig. 4. (a) I_{DS}-V_{GS} characteristics after endurance measurement up to 10^5 cycles (b) Normalized pull-in voltage (V_{PI}) and release voltage (V_{RL}) during 2×10^5 cycles. The release voltage moved toward the negative direction after 200 k cycles due to a welding between the beam and drain. (c) I_{DS}-V_{DS} characteristic of the printed MEM relay. (Extremely low R_{ON} of 3.69 Ω was extracted.).

stiction force seen during prolonged cycling (Figure 4b). The expected temperatures and dominant failure mechanisms are still under investigation. A small hysteresis window of 2 V was observed due to stiction force and pull-in mode operation. This window could potentially be further reduced by minimizing V_{DS} and introducing anti-stiction surface

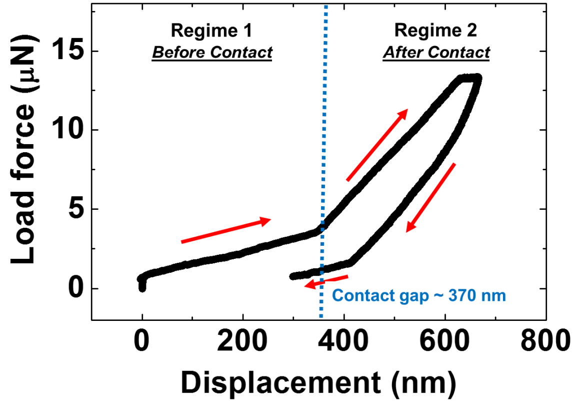

Fig. 5. Displacement versus applied force curve of the double-clamped beam as measured by nanoindentation. From the regime 1, spring constant (k_{eff}) could be extracted based on the fact that $F = k_{eff}\ x$(=displacement). [9].

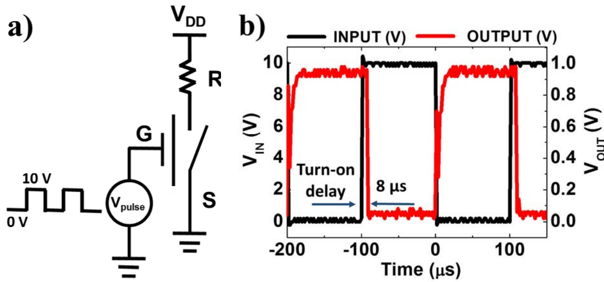

Fig. 6. (a) Schematic of relay inverter circuit with load resistor (100 kΩ) and V_{DD} of 1 V. (b) Dynamic behavior of the printed MEM inverter with 5 kHz square-wave pulse. (Pull-in delay of 8 μs during the channel traveling downward toward the drain).

treatments on the drain [24], [25]. The measured I_{DS} versus the drain voltage (V_{DS}) for a fixed V_{GS} of 10 V is shown in Figure 4c. An extremely low *on*-state resistance (R_{ON}) of 3.7 Ω for $V_{GS} > V_{PI}$ was achieved, showing excellent linearity with V_{DS} because the R_{ON}consists of two metallic components: first, a metal-metal contact resistance between the beam and drain and, second, the metallic channel resistance. The measured real spring constant of 7.78 N/m measured using a nanoindentor is well-matched with the calculated k_{eff} value using equation 4 with the design parameters. (Figure 5). This measurement also provides information for the contact gap from a change of the slope in displacement versus load force.

Dynamic behavior of the printed relay was also investigated by measuring transient characteristics in an inverter system as shown in Figure 6a. An external resistor (R_L of 100 kΩ) was connected in series with the drain electrode for an inverter setup that limits the maximum I_{DS} during *on*-state to prevent welding-related failure by joule heating. Figure 6b shows the AC input and output characteristics of the inverter for a 5 kHz square-wave input signal with an amplitude of 10 V. When V_{GS} was 0 V at the gate (*off-state*), the channel beam did not actuate toward the drain; V_{DS} was then V_{DD}, i.e., 1 V. When the beam was actuated down to close the circuit, the V_{DS} approaches 0 V since R_{ON} is much lower than R_L. During the transition between switching on/off states, a pull-in delay of 8 μs was observed; this is dominated by the mechanical delay, which is much larger than the intrinsic electrical *RC* delay because of extremely low *on*-state resistance and overlap capacitance values of the relay. Therefore, pull-in delay can be defined as below [13].

$$t_{delay} \propto \sqrt{\frac{m_{eff}}{k_{eff}}} \times \frac{V_{PI}}{V_{dd}} \tag{5}$$

where m_{eff} denotes the effective mass of transport. Therefore, a high k_{eff} and low V_{PI} can be achieved by introducing a double-clamped channel-beam and minimizing the gaps for improved high-frequency response, respectively. By using a beam with optimized stiffness, using a drain with high-aspect ratio, and implementing a relatively thin sacrificial layer, a delay below 10 μs was achieved using a V_{GS} of 10 V, thus delivering better dynamic behavior than previously reported work performed with a high V_{GS} of 20 V [9]. Also, the sharp ridge of the drain enhanced a turn-off delay to almost zero by minimizing the stiction force between the beam and drain. Although the MEM relay fabricated by conventional photolithography processes exhibited a shorter pull-in delay [26], the result was achieved from much mechanically stronger beam (Young modulus value of the beam ∼ 380 GPa) with a beam width and length of 25 μm and 15 μm, respectively, and a V_{PI} of 65 V.

During the dynamic behavior measurement, the required switching energy of ∼ 18 pJ which is lost during each cycle can be calculated using the following equation [27], [28],

$$E_{switch} \cong [\frac{\varepsilon A}{g - g_d}(1 + \gamma) + C]V_{PI}^2 \tag{6}$$

where E_{switch}, A, g, γ, C, and V_{PI} denote the switching energy, the actuation area, the actuation gap, the area proportionality factor, the load capacitance, and the supplied pull-in voltage, respectively. The small g_d is also an important parameter to minimize the mechanical strain distribution of the beam, because the maximum strain is directly proportional to the maximum deflection of the beam as defined below [13].

$$\varepsilon_{\max} \propto \frac{hz_{\max}}{L^2} \tag{7}$$

where h, z_{max} and L denote the thickness, maximum deflection, and length of the beam respectively. Since the length and height are limited by the minimum mechanical stiffness, to realize a freely suspended beam, optimization of the beam deflection is the most effective approach to enhance the endurance performance, minimizing structural fatigue.

VI. Conclusion

We successfully demonstrated and analyzed an inkjet-printed MEM relay with a double-clamped beam for achieving high-speed and reliable switching performance. By adopting the double-clamped beam and a 500 nm ridge on the drain, a strongly suspended beam and a reduced mechanical switching delay were realized without collapse or curling issues, even though relatively thin printed films were used for the

beam formation. The simulation results using COMSOL multiphysics predicted and supported the measured experimental values and distribution of the mechanical strain. Note that inkjet-printing has advantages in 1) enabling exploitation of the coffee ring to minimize contact area, thus ensuring minimal stiction during operation and reduced effective contact gap, and 2) rapid additively patterned thick-film formation; on the other hand, dimensional scaling is challenging due to the large feature sizes of inkjet-printing (~100 μm in this work). Also, for further reliable operation, printable materials having a high melting-point should be investigated because the high current density attributed to the low R_{ON} (~4 Ω) and the small contact area can accelerate welding-induced failures. Based on our results, we believe that the improved inkjet-printed MEM relays can be applicable to robust, low-cost and large area logic applications.

REFERENCES

[1] H. Yan *et al.*, "A high-mobility electron-transporting polymer for printed transistors," *Nature*, vol. 457, pp. 679–686, Feb. 2009.

[2] S. Chung *et al.*, "Flexible high-performance all-inkjet-printed inverters: Organo-compatible and stable interface engineering," *Adv. Mater.*, vol. 25, no. 34, pp. 4773–4777, Sep. 2013.

[3] H. Andersson, A. Manuilskiy, T. U. C. Lidenmark, S. Forsberg, and H.-E. Nilsson, "Inkjet printed silver nanoparticle humidity sensor with memory effect on paper," *IEEE J. Sensors*, vol. 12, no. 6, pp. 1901–1905, Jun. 2012.

[4] V. Subramanian *et al.*, "Progress toward development of all-printed RFID tags: Materials, processes, and devices," *Proc. IEEE*, vol. 93, no. 7, pp. 1330–1338, Jul. 2005.

[5] K. Kim *et al.*, "High-resolution electrohydrodynamic jet printing of small-molecule organic light-emitting diodes," *Nanoscale*, vol. 7, pp. 13410–13415, Jul. 2015.

[6] D.-H. Lien, Z.-K. Kao, T.-H. Huang, Y.-C. Liao, S.-C. Lee, and J.-H. He, "All-printed paper memory," *ACS Nano*, vol. 8, no. 8, pp. 7613–7619, Jul. 2014.

[7] H. L. Gomes *et al.*, "All-inkjet printed organic transistors: Dielectric surface passivation techniques for improved operational stability and lifetime," *Microelectron. Reliab.*, vol. 55, no. 8, pp. 1192–1195, Jul. 2015.

[8] S. Y. Cho, J. M. Ko, J.-Y. Jung, J.-Y. Lee, D. H. Choi, and C. Lee, "High-performance organic thin film transistors based on inkjet-printed polymer/TIPS pentacene blends," *Organic Electron.*, vol. 13, no. 8, pp. 1329–1339, Aug. 2012.

[9] E. S. Park, Y. Chen, K. T.-J. Liu, and V. Subramanian, "A new switching device for printed electronics: Inkjet-printed microelectromechanical relay," *Nano Lett.*, vol. 13, no. 11, pp. 5355–5360, 2013.

[10] S. Chung, M. A. U. Karim, M. Spencer, H.-J. Kwon, E. Alon, and V. Subramanian, "Exploitation of the coffee-ring effect to realize mechanically enhanced inkjet-printed microelectromechanical relays with U-bar-shaped cantilevers," *Appl. Phys. Lett.*, vol. 105, p. 261901, Dec. 2014.

[11] N. Tas, T. Sonnenberg, H. Jansen, R. Legtenberg, and M. Elwenspoek, "Stiction in surface micromachining," *J. Micromech. Microeng.*, vol. 6, no. 4, pp. 385–397, 1996.

[12] B. H. Lee *et al.*, "A mechanical and electrical transistor structure (METS) with a sub-2 nm nanogap for effective voltage scaling," *Nanoscale*, vol. 6, no. 14, pp. 7799–7804, Apr. 2014.

[13] H. Kam and F. Chen, *Micro-Relay Technology for Energy-Efficient Integrated Circuits*. New York, NY, USA: Springer, 2014.

[14] J. M. Gere and B. J. Goodno, *Mechanics of Materials*. USA: CL-Engineering, 2013.

[15] S. Pamidighantam, R. Puers, K. Baert, and H. A. C. Tilmans, "Pull-in voltage analysis of electrostatically actuated beam structures with fixed-fixed and fixed-free end conditions," *J. Micromech. Microeng.*, vol. 12, pp. 458–464, Jun. 2002.

[16] M. A. U. Karim, S. Chung, E. Alon, and V. Subramanian, "Stress-tolerant fully inkjet-printed reed relays," in *Proc. Solid-State Sensors, Actuat. Microsyst. (TRANSDUCERS)*, Jun. 2015, pp. 568–571.

[17] J.-H. Kim, Z. C. Y. Chen, S. Kwon, and J. Xiang, "Three-terminal nanoelectromechanical field effect transistor with abrupt subthreshold slope," *Nano Lett.*, vol. 14, no. 3, pp. 1687–1691, 2014.

[18] P. J. Yunker, T. Still, M. A. Lohr, and A. G. Yodh, "Suppression of the coffee-ring effect by shape-dependent capillary interactions," *Nature*, vol. 476, pp. 308–311, Aug. 2011.

[19] G. M. Rebeiz and R. M. Theory, *Design and Technology*. Hoboken, NJ, USA: Wiley, 2003.

[20] H.-H. Yang, M.-H. Seo, C.-H. Han, and J.-B. Yoon, "A new approach to control a deflection of an electroplated microstructure: Dual current electroplating methods," *J. Micromech. Microeng.*, vol. 23, p. 055016, Apr. 2013.

[21] J. Jeon, R. Nathanael, V. Pott, and T. J. K. Liu, "Four-terminal relay design for improved body effect," *IEEE Electron Device Lett.*, vol. 31, no. 5, pp. 515–517, May 2010.

[22] K. Akarvardar *et al.*, "Design considerations for complementary nanoelectromechanical logic gates," in *Proc. IEEE Int. Electron Devices Meeting (IEDM)*, Dec. 2007, pp. 299–302.

[23] T. J. K. Liu, J. Jeon, R. Nathanael, H. Kam, V. Pott, and E. Alon, "Prospects for MEM logic switch technology," in *Proc. IEEE Int. Electron Devices Meeting (IEDM)*, Dec. 2010, pp. 18.3.1–18.3.4.

[24] R. Maboudian, W. R. Ashurst, and C. Carraro, "Self-assembled monolayers as anti-stiction coatings for MEMS: Characteristics and recent developments," *Sens. Actuators A, Phys.*, vol. 82, nos. 1–3, pp. 219–223, 2000.

[25] M. Ramezani *et al.*, "Submicron three-terminal SiGe-based electromechanical ohmic relay," in *Proc. IEEE 27th Int. Conf. Micro Electro Mech. Syst. (MEMS)*, Jan. 2014, pp. 1095–1098.

[26] A. Verger, A. Pothier, C. Guines, P. Blondy, O. Vendier, and F. Courtade, "Nanogap MEMS micro-relay with 70 ns switching speed," in *Proc. IEEE 25th Int. Conf. Micro Electro Mech. Syst. (MEMS)*, Feb. 2012, pp. 717–720.

[27] H. Kam, T.-J. K. Liu, V. Stojanović, D. Marković, and E. Alon, "Design, optimization, and scaling of MEM relays for ultra-low-power digital logic," *IEEE Trans. Electron Devices*, vol. 58, no. 1, pp. 236–250, Jan. 2011.

[28] C. Pawashe, K. Lin, and K. J. Kuhn, "Scaling limits of electrostatic nanorelays," *IEEE Trans. Electron Devices*, vol. 60, no. 9, pp. 2936–2942, Sep. 2013.

Seungjun Chung received the B.S. degree in electrical engineering from Korea University, Seoul, South Korea, in 2006, and the Ph.D. degree in electrical engineering from Seoul National University, South Korea, in 2012. He was with the Prof. Subramanian's Group in electrical engineering, University of California at Berkeley, Berkeley, CA, USA, as a Post-Doctoral Researcher until 2016. He is currently a BK Assistant Professor with the Department of Physics and Astronomy, Seoul National University.

During his Post-Doctoral Research, he intensively investigated novel inkjet-printed systems, including microelectromechanical relays, transparent oxide thin-film transistors, and resistive memory devices. His current research interests are in device physics, manufacturing of low-cost thin film micro/nanoelectronics, and nanomaterials for the next generation electronics.

Muhammed Ahosan Ul Karim received the B.S. and M.S. degrees in electrical engineering from the Bangladesh University of Engineering and Technology in 2007 and 2010, respectively. He is currently pursuing the Ph.D. degree with the University of California at Berkeley, Berkeley, CA, USA. His works on the compact modeling of the bulk MOSFETS, UTBSOI MOSFETs, and FinFETs have contributed to the BSIM compact model family. He is involved in printed MEMS, including process development, device architecture, materials characterization, and modeling. His research interests include solution processed electronics, additive manufacturing, energy conversion and storage, and printed MEMS.

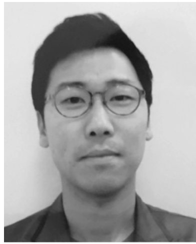

Hyuk-Jun Kwon received the bachelor's degree in mechanical engineering from Korea University, South Korea, in 2007, the master's degree in mechanical engineering from KAIST, South Korea, in 2009, and the Ph.D. degree from the University of California at Berkeley, Berkeley, CA, USA, in 2015. After working for the next generation displays as a Research and Development Staff with the Materials and Devices Research Center, Samsung Advanced Institute of Technology from 2009 to 2011, he joined the Laser Thermal Laboratory, Department of Mechanical Engineering, University of California at Berkeley in 2011. He was a Post-Doctoral Fellow in 2015.

He is currently a Process Engineer with the Corporate Technology Development of Lam Research. He specializes in heat transfer based on laser process and device physics for flexible electronics. His research at the LTL was in laser processing and micro/nanomachining for the fabrication of flexible/wearable electronics using 2-D materials and 2-D random networks. His current research interests are in shallow doping and surface modification using ultrafast-pulsed lasers for the next generation process of semiconductors.

William Scheideler received the B.S. degree in electrical engineering and the B.S. degree in biomedical engineering from Duke University in 2013. He is currently pursuing the Ph.D. degree with the University of California at Berkeley, Berkeley, CA, USA, where he is involed in developing solution-processed metal oxides and printing methods for additive manufacturing of transparent electronics. His research interests include gravure printing, metal oxide transistors, biomedical imaging, and scalable nanomanufacturing.

Vivek Subramanian (M'94) received the Ph.D. degree in electrical engineering from Stanford University in 1998. He co-founded Matrix Semiconductor, Inc., in 1998. Since 2000, he has been with the University of California at Berkeley, Berkeley, CA, USA, where he is currently a Professor of Electrical Engineering and Computer Sciences. His current research focuses on printed electronics for display, low-cost logic, and sensing applications. He received the Paul Rappaport Award for the best paper in the IEEE ELECTRON DEVICES SOCIETY JOURNAL, the IEEE Device Research Conference, and the IMAPS best paper awards, the 2015 IEEE Kiyo Tomiyasu Award, and the Outstanding Teaching Award from the Electrical Engineering and Computer Science Department, University of California, Berkeley.